Published in final edited form as:
J Comp Neurol. 2012 December 15; 520(18): 4168–4183. doi:10.1002/cne.23145.

Neuroanatomy of melanocortin-4 receptor pathway in the lateral hypothalamic area

Huxing Cui[1,2], **Jong-Woo Sohn**[2], **Laurent Gautron**[2], **Hisayuki Funahashi**[3], **Kevin W. Williams**[2], **Joel K. Elmquist**[1,2], and **Michael Lutter**[1,4]

[1]Department of Psychiatry, The University of Texas Southwestern Medical Center, Dallas, Texas, 75390-9127

[2]Departments of Internal Medicine and Pharmacology, Division of Hypothalamic Research, The University of Texas Southwestern Medical Center, Dallas, Texas, 75390-9127

[3]Department of Anatomy, Showa University School of Medicine, 1-5-8 Hatanodai, Shinagawa-ku, Tokyo, 142-8555 Japan

Abstract

The central melanocortin system regulates body energy homeostasis including the melanocortin-4 receptor (MC4R). The lateral hypothalamic area (LHA) receives dense melanocortinergic inputs from the arcuate nucleus of hypothalamus and regulates multiple processes including food intake, reward behaviors and autonomic function. Using a mouse line in which green fluorescent protein (GFP) is expressed under control of MC4R gene promoter, we systemically investigated MC4R signaling in the LHA by combining double immunohistochemistry, electrophysiology and retrograde tracing techniques. We found that LHA MC4R-GFP neurons co-express neurotensin as well as the leptin receptor but not with other peptide neurotransmitters found in the LHA including orexin, melanin concentrating hormone and nesfatin-1. Furthermore, electrophysiological recording demonstrated that leptin, but not the MC4R agonist melanotan II, hyperpolarizes the majority of LHA MC4R-GFP neurons in an ATP-sensitive potassium channel-dependent manner. Retrograde tracing revealed that LHA MC4R-GFP neurons do not project to the ventral tegmental area, dorsal raphe nucleus, nucleus accumbens and spinal cord, and only limited number of neurons project to the nucleus of solitary tract and parabrachial nucleus. Our findings provide new insight into MC4R signaling in the LHA and its potential implication in homeostatic regulation of body energy balance.

Keywords

Leptin receptor; neurotensin; electrophyiosology; orexin; melanin concentrating hormone; nesfatin

Introduction

Due to its increasing prevalence and serious co-morbidities including diabetes, cancer and cardiovascular diseases, obesity has become a major health concern facing to the developed countries (WHO, 2004). Our understanding of the mechanisms underlying body weight regulation has dramatically improved since the discovery that several peripheral hormones, including insulin, leptin and ghrelin, regulate energy balance through signaling in the brain

Corresponding Author: 200 Hawkins Dr., B020 ML, Iowa City, IA 52242, Ph: 319-335-7256, Michael-Lutter@uiowa.edu.
[4]Present Address: Department of Psychiatry, University of Iowa, 200 Hawkins Dr. B020 ML, Iowa City, IA 52242.

Conflict of Interest: None

(Saper et al., 2002; Schwartz et al., 2000; Zhang et al., 1994). It is now clear that the central melanocortin system is critical for the integration of multiple peripheral signals to maintain body weight homeostasis (Bjorbaek and Hollenberg, 2002; Cone, 2005; 2006; Elmquist et al., 1999; Schwartz et al., 2000; Shimizu et al., 2007).

The central melanocortin system consists of two G protein coupled receptors: the melanocortin-3 receptor (MC3R) and melanocortin-4 receptor (MC4R) (Cone, 2006). An endogenous ligand for both receptors is α-melanocyte-stimulating hormone (α-MSH), which is derived from the precursor proopiomelanocortin (POMC). The central melanocortin system is unique in that it also features an endogenous antagonist agouti-related protein (AgRP). AgRP and α-MSH are synthesized in distinct population of neurons within the arcuate nucleus of the hypothalamus (ARH) and project diffusely throughout the brain (Bagnol et al., 1999; Cone, 2005; Schwartz et al., 2000). Mutations in the *MC4R* gene are found in up to 5% of human patients with morbid obesity have mutations in the *MC4R* gene (Santini *et al.*, 2009). Numerous studies in rodents have also clearly demonstrated that activation of MC4Rs suppresses feeding and increases energy expenditure, whereas pharmacologic or genetic inhibition of MC4Rs has the opposite effects (Balthasar et al., 2005; Benoit et al., 2000; Chen et al., 2000; Fan et al., 1997; Marsh et al., 1999). Thus, characterizing neural circuits affected by MC4R signaling will facilitate our knowledge on how the brain integrates peripheral signals to maintain body energy balance.

Consistent with the broad projections of ARH POMC/AgRP neurons in the central nervous system (CNS), MC4Rs are widely expressed in many regions of the rodent brain (Kishi et al., 2003; Liu et al., 2003; Mountjoy et al., 1994). Of these regions, the paraventricular nucleus (PVH) and lateral hypothalamic area (LHA) are of particular interest since they receive dense inputs from leptin responsive POMC/ AGRP neurons (Elias *et al.*, 1999) and express MC4Rs (Kishi *et al.*, 2003; Liu *et al.*, 2003). While it is clear that MC4Rs are expressed in these regions, their specific functions are not completely understood. One study utilizing a Cre/loxP genetic technique demonstrated that MC4R signaling in SIM1-expressing neurons of the PVH and/or amygdala is essential for homeostatic regulation of energy balance primarily by affecting food intake but not energy expenditure (Balthasar *et al.*, 2005). Several neuroanatomical studies have shown that PVH MC4R-positive neurons colocalize with several neuropeptides, including corticotropin-releasing hormone, oxytocin and thyrotropin-releasing hormone, and project to multiple regions including the nucleus of the solitary tract (NTS), the spinal cord and the median eminence of hypothalamus (Ghamari-Langroudi et al., 2011; Harris et al., 2001; Liu et al., 2003; Lu et al., 2003).

In contrast to our understanding of the PVH MC4R pathway, relatively little is known about the physiological importance of MC4Rs expressed in the LHA. The LHA has long been appreciated for its crucial role in the regulation of feeding, motivational behaviors and autonomic function (Bernardis and Bellinger, 1993b). A recent study demonstrated that pharmacological blockade of LHA MC4R signaling does not significantly alter food intake when animals fed regular chow (RC) (Kim *et al.*, 2000). However a separate study found that over-expression of the melanocortin receptor antagonist Agouti in the LHA induces significant hyperphagia and body weight gain when mice were placed on a palatable high fat diet (HFD) (Kas *et al.*, 2004). This suggests that the MC4R signaling in LHA regulates hedonic drive of feeding and might be responsible for exacerbated diet-induced obesity seen in MC4R-null mice (Butler *et al.*, 2001; Srisai *et al.*, 2011).

In the current study we systemically examined the neuroanatomical and electrophysiological characteristics of MC4R neurons in the LHA and provide new insights into the understanding of its potential physiological function.

Materials and Methods

Animals

Mice in which GFP expression is under control of MC4R gene promoter (MC4R-GFP) were obtained for neuroanatomical studies (Liu *et al.*, 2003). As reported previously, nearly all of the MC4R-GFP positive neurons in this line co-express MC4R mRNA including neurons shown in a representative photograph of the perifornical area (Figure 5 in the original paper). Hence, we believe that the MC4R-GFP line faithfully identifies MC4R-expressing neurons in the LHA. Mice were housed in the University of Texas Southwestern Medical Center (UTSW) vivarium in a temperature-controlled environment (lights on: 06:00–18:00) with *ad lib* access to water and standard chow (SC) (4% fat diet #7001, Harlan-Teklad, Madison, WI). All animal procedures were performed in accordance with UTSW Institutional Animal Care and Use Committee guidelines.

Antibody Characterization

The antibodies used in the present study are all commercially available and have been tested by different laboratories. Their key features are summarized in Table 1.

1. Chicken anti-GFP polyclonal antiserum (Aves, Tigard, OR). The manufacturer has previously analyzed the antibody by Western blot by using transgenic mice expressing GFP. Western blot analysis produced a single band of 28 kDa. Furthermore, Zhao and colleagues (Zhao *et al.*, 2008) showed that the antiserum produces no staining in the brain of wild-type mice, but did stain brain sections of transgenic mice expressing GFP. In our samples, the antiserum produced comparable staining to that obtained with the rabbit antiserum described in the original paper (Liu *et al.*, 2003). Also, this antibody is included in the JCN Antibody Database and frequently used in many other studies for immunohistochemical detection of GFP (Bulloch et al., 2008; Xu et al., 2010; Yee et al., 2009)

2. Rabbit anti-neurotensin (NT) antiserum (ImmunoStar, Hudson, WI) was quality control tested by manufacturer using standard IHC methods. The antiserum demonstrates significant labeling of rat amygdala using indirect immunofluorescent and biotin/avidin-HRP techniques. Staining was completely eliminated by pretreatment of antibody with diluted NT solution. Furthermore, this antibody was successfully used to detect NT in a newly developed hypothalamic cell lines that constantly expresses NT by immunocytohistochemistry and the staining was disappeared by preincubation with NT peptides (Cui *et al.*, 2005). Additionally, this antibody was also used to characterize afferent ventral tegmental area NT fibers and the staining produced identical somatic NT expression patterns in colchicine-treated brain sections compared to NT mRNA expression (Geisler and Zahm, 2006). In present study we also observed nearly identical somatic NT expression patterns in whole brain sections of colchicine-treated mouse compared to NT mRNA expression that readily available in Allen Brain Atlas Database (data not shown). The antibody is registered in the JCN Antibody Database and several more studies have successfully used this antibody to detect NT in different tissues (Moore *et al.*, 2002; Shroyer *et al.*, 2005; Zahm *et al.*, 2011)

3. pSTAT3 antibody specificity was tested using an enzyme-linked immunosorbent assay, demonstrating specific binding of the antibody with a phosphorylated STAT3 peptide and the absence of binding when incubated with the nonphospho-STAT3 peptide. As well, preabsorption of pSTAT3 antiserum using a synthetic phospho-STAT3 peptide completely blocked antibody reactivity in pSTAT3-expressing tissue sections (Cell Signaling Technology, Danvers, MA).

Furthermore, this antibody was successfully used for characterizing leptin receptor reporter mouse line in which leptin-induced pSTAT3 IHC signals were mainly observed in leptin receptor-positive cells in the brain (Scott *et al.*, 2009). This antibody is also registered in the JCN Antibody Database.

4. c-Fos (CALBIOCHEM, Gibbstown, NJ) antibody was raised against a synthetic peptide corresponding to amino acids 4–17 of human c-Fos. Western blot analysis from previous characterization indicated that the antibody recognizes 55-kDa c-Fos and 62-kDa v-Fos proteins but does not cross-react with the 39-kDa Jun proteins (manufacturer's technical information). This antibody is also included in the JCN antibody database and has been successfully used to detect CNS c-Fos induction by IHC (Harrison *et al.*, 2008; Reznikov *et al.*, 2008).

5. Rabbit polyclonal antiserum against fluorogold (FG) (Chemicon, now Millipore, Billerica, MA). Elias and colleague (Elias *et al.*, 1999) showed that this antibody stains FG injections site and retrogradely labeled neurons in the rat brain. As well, in present study we observed clear staining in FG-injected mouse brain sections but not in the brain sections of animals without FG injections (data not shown), indicating that this antibody has no cross-reactivity to any of endogenous antigens in the mouse brain. The antibody is registered in the JCN Antibody Database and has been frequently and successfully used in many other studies (Gautron et al., 2010b; Lefler et al., 2008; Li et al., 2006)

6. Goat polyclonal antiserum against cholera toxin b subunit (CTb) (List Biological Laboratories, Campbell, CA). Kishi and colleagues (Kishi *et al.*, 2000) demonstrated that this antibody stains CTb injection sites and retrogradely labeled neurons in the rat brain. As well, in present study this antibody clearly stained CTb injection sites and retrogradely labeled neurons in the mouse brain, but it did not stain brain sections from animals without CTb injections (data not shown), indicating that this antibody has no cross-reactivity to any of endogenous antigens in the mouse brain. The antibody is registered in the JCN Antibody Database and has been frequently and successfully used in many other studies (Al-Khater *et al.*, 2008; Howorth *et al.*, 2009; Wittmann *et al.*, 2009)

7. Melanin Concentrating Hormone (MCH) (Phoenix Pharmaceuticals, Burlingame, CA) antibody was raised in rabbit and had no cross-reactivity to other peptides including orexin A and B, agouti-related peptide, α-melanocyte stimulating hormone and neuropeptide Y as provided by manufacturer. As previously reported, in present study this antibody produced clear somatic staining only in the LHA and which was completely different from orexin IHC signal. The antibody is registered in the JCN Antibody Database and has been successfully used to detect endogenous MCH in many other studies (Berman et al., 2009; Glavas et al., 2008; Shin et al., 2008)

8. Orexin antibody (Santa Cruz Biotechnology, Santa Cruz, CA). Florenzano and colleagues (Florenzano *et al.*, 2006) have previously shown that this antibody stains orexin-A specifically in the LHA and this immunoreactivity is prevented by preabsorption with orexin peptide, indicating this antibody recognizes endogenous orexin-A. Importantly, this antibody produced no signals in orexin knockout mice (Liu *et al.*, 2008), suggesting no cross-reactivity to other endogenous antigens. The antibody is registered in the JCN Antibody Database and has been successfully used to detect endogenous orexin in many other studies (Florenzano *et al.*, 2006; Glavas *et al.*, 2008; Liu *et al.*, 2011).

9. Nesfatin-1 antiserum (Phoenix Pharmaceuticals) cross-reacts 100% with rat nesfatin-1 (1–82) and does not cross-react with the following peptides: nesfatin-1

(1–45, human), nesfatin-1 (47–82, human), agouti-related peptide (83–132, human), α-melanocyte stimulating hormone, orexin A (human, rat, mouse), neuropeptide Y (rat), ghrelin (rat, mouse), and obestatin (rat, mouse). By combining in situ hybridization, immunohistochemistry and western blotting, Garcia-Galiano *et al* (2010) have characterized brain expression of nesfating-1 in details. Western blot analysis resulted single band that corespond to 42 KDa molecualr weight of nesfatin-1 precursor protein nucleobing-2 and IHC produced identical immunostaining to that mRNA expression of nucleobindin-2 (Garcia-Galiano *et al.*, 2010). In the present study, this nesfatin-1 antibody produced identical staining as previously reported (Brailoiu et al., 2007; Kohno et al., 2008; Oh et al., 2006).

Stereotaxic surgery for retrograde neuronal tracing

Surgical procedure was followed as previously described (Chamberlin *et al.*, 1998; Gautron *et al.*, 2010a). Briefly, MC4R-GFP mice were anesthetized with ketamine HCl/xylazine HCl (80:12 mg/kg, i.p.) and restrained in a Kopf (Tujunga, CA) stereotaxic apparatus. A small hole was drilled into the skull under aseptic conditions. A glass micropipette connected to an air pressure injector system or iontophoresis machine was positioned via the stereotaxic manipulator. Approximately 50–100 nL of retrograde tracer, fluorogold (Fluorochrome, CO, USA) or choleratoxin subunit B (CTb) (List Biological Laboratories), was slowly administered into the ventral tegmental area (VTA) (−3.2 mm from bregma, 1.1 mm lateral with 10 degree injection arm, −4.3 mm from the surface of the cortex), the dorsal raphe (DR) (−4.6 mm from bregma, 0.1 mm lateral, −2.7 mm from the skull), the nucleus accumbens-shell (NAc-shell) (1.5 mm from bregma, 1.5 mm lateral with 10 degree injection arm, −4.2 mm from the surface of the cortex), the nucleus of solitary tract (NTS) (+0.16 from the obex, ±0.23 mm lateral, −0.36mm from the surface of the brainstem and the parabrachial nucleus (PBN) (−5.2 mm from bregma, 1.3 mm lateral, −2.8 mm from the cerebellar cortex). For spinal cord injection, the T6–T7 facet joint was removed by surgical instrumentation and retrograde tracer FG was unilaterally injected by air pressure injection system. After injection, the glass micropipette was removed and the incision was closed with surgical staples. Mice were allowed to recover for 5–7 days post surgery and then perfused with 4% paraformaldehyde (PFA) and brain sections were processed for double fluorescent immunohistochemistry for GFP and tracers.

Fluorescent double immunohistochemistry (IHC)

To enhance labeling of cell bodies with immunohistochemistry, MC4R-GFP mice were treated with intracerebroventricular (ICV) colchicine (10 ug) 48 hours prior to perfusion. For leptin-induced phospho-STAT3 and melanotan II (MT-II)-induced c-Fos experiments, MC4R-GFP mice were treated with intraperitoneal (IP) leptin (5 mg/kg, National Hormone and Peptide Program, Harbor-UCLA Medical Center, Torrance, CA), IP MT-II (3 mg/kg, Bachem, Torrance, CA IP), ICV leptin (1.5 ug), or ICV MTII (1 ug) as noted, 2 hours prior to perfusion. Mice were transcardially perfused with 4% PFA and cryopreserved in 20% sucrose. Brains were then sectioned into 30 micron coronal sections (collecting 1:5 sections) and stored in cryoprotectant at −20 °C until use. Brain sections were blocked and permeabilized with 3% normal donkey serum (NDS, Jackson Immuno Research, West Grove, PA), 0.3% Triton X-100 in PBS for 30 minutes at room temperature (RT), rinsed with PBS and incubated with primary antibodies (diluted in 3% NDS, 0.3% Tween-20 in PBS) at room temperature for 2–3 hours or at 4 °C for overnight. For leptin-induced pSTAT3, brain sections were treated with 1% NaOH, 1% H_2O_2 in distilled water for 20 minutes at room temperature, rinsed with PBS 3 times for 10 minutes each, incubated with 0.3% Glycine in PBS for 10 minutes, rinsed with PBS 3 times for 10 minutes each, incubated with 0.03% SDS in PBS for 10 minutes, blocked in 3% NDS, 0.3% Triton X-100

in PBS for 30 minutes at room temperature and then incubated with primary antibody for 24 hours at room temperature plus additional 48 hours at 4 °C. Images were first taken by fluorescent microscopy (Nikon Eclipse, 80i) and co-localization was determined by confocal microscope scanning (LSM510-META, Zeiss, Thornwood NY). Cells counts for pSTAT3 and GFP positive neurons were made in mid-dorsal lateral hypothalamus from three consecutive sections with the highest abundance of GFP expression.

Electrophysiological recording

To examine the role of leptin receptor in MC4R-positive LHA neurons, we examined the effect of leptin (100 nM) on the membrane potential of GFP-positive LHA neurons from MC4R-GFP transgenic mice. As described previously (Hill et al., 2008a; Williams et al., 2010), 4–10 weeks old mice were deeply anesthetized with chloral hydrate and transcardially perfused with a modified ice-cold artificial cerebrospinal fluid (ACSF, described below), in which an equiosmolar amount of sucrose was substituted for NaCl. The mice were then decapitated, and the entire brain was removed and immediately submerged in ice-cold, carbogen-saturated (95% O2 and 5% CO2) ACSF (126 mM NaCl, 2.5 mM KCl, 1.2 mM MgCl2, 2.4 mM CaCl2, 1.25 mM NaH2PO4, 26 mM NaHCO3, and 10 mM glucose). Coronal sections (200μM) were cut with a Leica VT1000S Vibratome and then incubated in oxygenated ACSF at 32°C for at least 1 h before recording. Slices were transferred to the recording chamber and allowed to equilibrate for 10–20 min prior to recording. The slices were bathed in oxygenated ACSF (32°C–34°C) at a flow rate of approximately 2 ml/min. Epifluorescence was briefly used to target fluorescent cells, at which time the light source was switched to infrared differential interference contrast imaging to obtain the whole-cell recording using Zeiss Axioskop FS2 Plus (Carl Zeiss; Jena, Germany) equipped with a fixed stage and a Hamamatsu C2741-60 charged-coupled device camera (Hamamatsu photonics; Hamamatsu city, Japan). Membrane potentials were recorded in the current clamp mode using an Axopatch 700B amplifier (Molecular Devices; Sunnyvale, CA, USA), low-pass filtered at 1 kHz, digitized at 10 kHz and analyzed offline on a PC with pCLAMP programs (Molecular Devices), Origin (Microcal; Piscataway, NJ, USA) or IgorPro (Wavemetrics; Lake Oswego, OR, USA). Recording electrodes had resistances of 2.5–5 MΩ when filled with the K-gluconate pipette solution which contains 120 mM K-gluconate, 10 mM KCl, 10 mM HEPES, 5 mM EGTA, 1 mM CaCl2, 1 mM MgCl2, and 5 mM Mg-ATP adjusted to pH 7.3.

MT-II and Leptin-induced c-Fos activation on LHA orexin neurons

Eighteen 8–9 week old C57BL/6 male mice (Jackson Laboratory, Bar Harbor, ME) were used for the study. One cohort of mice received IP injection of saline, MTII (3 mg/kg) or leptin (5 mg/kg), respectively (n=3/group), at 1800 (ZT18) just before lights off and fresh brains were collected by decapitation at 2000 (ZT20). Likewise, a second cohort of mice received IP injection of saline, MTII (3 mg/kg) or leptin (5 mg/kg), respectively (n=3/group), at 0600 AM (ZT6) just before lights on and fresh brains were collected by decapitation at 0800 (ZT8). Brains were post-fixed in 4% PFA at 4 °C for 48 hours, cryopreserved in 20% sucrose solution at 4 °C for 24 hours, and then cut into 5 series of 30 um sections. Brian sections were then stained for c-Fos and orexin by indirect biotin/avidin-HRP techniques as previously reported (Elias *et al.*, 1999).

Photomicrograph productions

Adobe Photoshop CS2 was used to combine drawings and digital images into plates. The contrast and brightness of images were adjusted when necessary. In addition, red-green fluorescence images were converted to magenta-green for color-blind readers.

Statistics

GraphPad Prism 5 software (GraphPad Software Inc., San Diego, CA) was used to perform statistical analyses. $P < 0.05$ was considered to be statistically significant.

Results

Neurochemical characterization of LHA MC4R-positive neurons

A previous study using *in situ* hybridization demonstrated low to moderate expression of MC4Rs in the LHA of the rat (Kishi *et al.*, 2003). In order to facilitate neuroanatomical studies of MC4R, a mouse line expressing tau-conjugated GFP under the control of the MC4R promoter (MC4R-GFP) was previously generated and validated (Liu *et al.*, 2003). This line has also been used for other neuroanatomical studies (Gautron *et al.*, 2010b). Utilizing this mouse line, we confirmed the expression of MC4R-GFP-positive neurons mainly in the dorsal LHA (Fig. 1A, F) as well as in the perifornical area (PFA) (Fig. 1H). The LHA is comprised of a heterogeneous cell population expressing multiple neurotransmitters. In order to determine the neurochemical phenotype of LHA MC4R-positive neurons, we carried out a series of co-localization studies to determine which neurotransmitters are expressed in LHA MC4R-GFP neurons. Dual-label fluorescent IHC demonstrated that LHA MC4R-GFP positive neurons are completely distinct from orexin, melanin concentrating hormone (MCH) (Fig. 1A, B), and nesfatin-1 expressing neurons (Fig 1C, D). In contrast, MC4R-GFP was co-expressed with the peptide neurotransmitter neurotensin (NT) in both dorsal LHA (Fig. 1E, F) and PFA (Fig 1E, H). Schematic drawing of distribution of NT, MC4R-GFP and double-positive cells in mid-dorsal LHA and PFA is shown in figure 1I. Detailed counting of NT, GFP and double-positive cells revealed that ~75% of MC4R-GFP neurons co-express with NT in the LHA and PFA (Table 2a). Importantly, after observing the colocalization of MC4R-GFP and NT within the LHA, we surveyed the entire brain and did not observe additional significant co-localization in any additional sites (data not shown).

Co-localization of LHA MC4R-GFP neurons with leptin-induced pSTAT3

Leinninger and colleagues recently identified a population of LHA neurons expressing the active form of the leptin receptor (LepRb), which is also distinct from orexin and MCH but co-localized with GAD67, a marker of GABAergic neurons (Leinninger *et al.*, 2009). We have previously shown that perifornical MC4R-GFP neurons co-express GAD67 (Liu *et al.*, 2003). These similarities in neurochemical phenotype between LHA LepRb-positive neurons and LHA MC4R-GFP neurons led us to hypothesize that LHA MC4R/NT/GAD67-positive neurons might co-express LepRb as well. To test this model, we conducted dual-label IHC for leptin-induced pSTAT3 and GFP in our MC4R-GFP mouse line. As predicted, there was a clear co-localization between MC4R-GFP neurons and pSTAT in the middorsal portions of LHA after leptin treatment (Fig. 2A, B). A schematic drawing of the distribution of pSTAT3, MC4R-GFP and double-positive cells in mid-dorsal LHA and PFA is shown in Figure 2C. Detailed counting of pSTAT3, GFP and double-positive cells revealed that ~80% of MC4R-GFP neurons co-express with pSTAT3 (Table 2b). In addition to the LHA, colocalization was also observed in the posterior hypothalamus and lateral periaqeductal grey (data not shown). Additionally, to understand the pharmacological effects of both MC4R and LepRb signaling within the LHA, we performed immunohistochemistry for c-Fos, a commonly used marker of neuronal activation (Kaczmarek and Nikolajew, 1990). MC4R-GFP mice were treated with either MC4R agonist (MTII) or leptin. Administration of either MTII or leptin (both ICV and IP) failed to induce c-Fos activation in LHA MC4R-GFP neurons (data not shown).

Electrophysiological recording of LHA MC4R-GFP neurons stimulated by both leptin and MTII

To further characterize the role of MC4R and leptin signaling within the LHA, we tested the electrophysiological responses of individual LHA MC4R-GFP neurons to leptin and MTII. We assessed membrane potential in neurons in the current clamp mode. The average resting membrane potential was −45.7 ± 1.7 mV in 16 cells. In 10 cells, leptin (100 nM) hyperpolarized the membrane potential by −8.6 ± 1.4 mV (Fig 3A–B). In the remaining 6 cells, leptin did not significantly alter the membrane potential (−0.2 ± 0.5 mV) (Fig 3C). The leptin-induced hyperpolarization lasted for approximately 10 min and was completely reversed by subsequent application of tolbutamide (200 uM, a specific KATP channel blocker) (Fig 3A–B). These results suggest that leptin directly inhibits a subpopulation of LHA MC4R-GFP neurons by activating KATP channels. Conversely, MTII (100 nM) had no effect on membrane potential in all LHA MC4R-GFP neurons recorded (Fig. 3D). These results suggest that leptin inhibits the firing of MC4R-GFP neurons in the LHA.

Potential innervation of LHA MC4R-GFP neurons

Next we sought to determine the innervation pattern of LHA MC4R-GFP neurons. Recent work by Leinninger and colleagues (Leinninger *et al.*, 2009) has shown that LHA LepRb neurons mainly project to the ventral tegmental area (VTA) and dorsal raphe (DR). Since one third of leptin-induced pSTAT3 neurons in the LHA were colocalized with MC4R-GFP, we hypothesized that LHA MC4R-GFP neurons might project to VTA and/or DR as well. To test this possibility, we injected retrograde tracer into these two brain regions of MC4R-GFP mice and brain sections were processed for double IHC for the GFP and tracer focusing on the LHA. Four successfully targeted cases were obtained for the VTA and representative photography of injection site is shown in Fig 4A. While many of LHA neurons were labeled with tracer as predicted, none of the neurons were GFP-positive (Fig 4B), suggesting that LHA MC4R-GFP neurons do not project to the VTA. For the DR, we obtained three successful injection cases and representative photography of injection site is shown in Fig 4C. While some of the LHA neurons were clearly labeled with retrograde tracer after successful injection into the DR, but none of the neurons were colocalized with GFP (Fig 4D), again suggesting that LHA MC4R-GFP neurons do not project to the DR as well. Additionally, since it has been reported that hedonic overconsumption of palatable high fat diet was observed in mice with overexpression of MC4R antagonist Agouti solely in the LHA (Kas *et al.*, 2004), we hypothesized that LHA MC4R-GFP neurons might project to nucleus accumbens (NAc) which has long been believed as a brain reward center that might regulate hedonic drive of feeding. To test this possibility, we injected the retrograde tracer fluorogold (FG) into the NAc-shell, which receives innervations from LHA neurons (Kelley *et al.*, 2005). Four successful cases were obtained and, as shown in Fig 4E, injection sites included the NAc-shell with extension into the adjacent core region. For all four successfully injected cases, only a few LHA neurons were labeled with tracer and none of them were colocalized with GFP signal (Fig 4F), which indicates that LHA MC4R-GFP neurons do not project to the NAc.

To further explore potential targets of LHA MC4R-GFP neurons, we injected tracer into the nucleus tractus solitarius (NTS), parabrachial nucleus (PBN), and spinal cord, which all have been previously shown to be innervated by LHA neurons (Haring and Davis, 1983; Kelly and Watts, 1998; Moga et al., 1990; Tokita et al., 2009; Zheng et al., 2005). We obtained three successful injection cases for the NTS and representative injection is shown in Fig 5A. For all three successfully NTS-injected cases, retrograde tracer CTb-labeled neurons were clearly observed in the LHA (Fig 5B), but only occasional neurons (< 8%) were colocalized with GFP signal (Fig 5C), indicating that the majority of LHA MC4R-GFP neurons do not project to the NTS. Since it has previously shown that the PBN is densely

innervated by LHA NT-positive neurons (Moga *et al.*, 1990), the PBN was also considered as a possible target for LHA MC4R-GFP neurons. In all six of the successfully injected cases, LHA neurons were intensively labeled by tracer (Fig. 5G, 5H, 5I). However, we only observed a few neurons that were double positive for tracer and GFP signal (< 12%), indicating that the PBN is not a major target of LHA MC4R-GFP neurons. For the spinal cord, retrograde tracer FG was injected into thoracic spinal cord (T6–T7). In the two successfully injected cases (Fig. 5D, 5E, 5F), considerable numbers of neurons in the LHA were labeled with FG as predicted, but none of them were GFP-positive, indicating that LHA MC4R-GFP neurons do not project to the spinal cord. Since it has been reported that PVH MC4R neurons project to both NTS and spinal cord (Ghamari-Langroudi *et al.*, 2011), we further analyzed PVH MC4R-GFP neurons in our successfully injected cases as a positive control experiment. Indeed, we confirmed clear projections of PVH MC4R-GFP neurons to both NTS and spinal cord in all of cases studied (data not shown).

MTII- and leptin-induced c-Fos on LHA orexin neurons

In addition to the VTA and DR, orexin neurons (also known as hypocretin) in the LHA have been reported to be a direct target of LHA LepRb neurons through a local circuit (Leinninger *et al.*, 2009; Louis *et al.*, 2010a). Furthermore, NT-positive LHA neurons have also been shown to project to the VTA as well as locally to orexin neurons within the LHA (Leinninger *et al.*, 2011). Because we had already ruled out the VTA as a potential target for LHA MC4R-GFP neurons, we tested the possibility that LHA MC4R-GFP neurons project to orexin neurons as well. Unfortunately because both MC4R-GFP and orexin neurons are interspersed within the LHA, we could not test this hypothesis using conventional retrograde tracing technique. Therefore, we utilized a complementary pharmacological approach to determine if the MC4R agonist MTII or leptin could affect orexin neuron activity using c-Fos IHC as a surrogate marker of activation. Orexin neurons display a diurnal activity pattern (Estabrooke *et al.*, 2001), therefore we preformed this experiment at two different time points, ZT8 and ZT20. As expected, in the saline-injected groups, the percentage of c-Fos expression in orexin neurons was significantly higher during the early dark phase (ZT20) compared to the early light phase (ZT8) (Fig 6A–F, table 3). Both MTII and leptin increased c-Fos expression in orexin neurons at ZT8 (Fig 6G–L, table 3), while no differences in c-Fos levels were detected between groups at ZT20 (Fig 6G–L, table 3).

Discussion

In the present study, we investigated anatomic and physiological properties of neurons in the LHA expressing MC4Rs. We found that LHA MC4R-GFP neurons co-express the anorexigenic peptide NT and the long form of LepRb, but not orexin, MCH or Nesfatin-1. While this population of neurons had no electrophysiological response to the MC4R agonist MTII, we found that most of the LHA MC4R-GFP neurons are inhibited by leptin. We were unable to identify the direct targets of LHA MC4R-positive neurons as they do not project to any of the brain regions we tested including NAc, VTA, DR, NTS, PBN and spinal cord. However, we provide pharmacological evidence supporting a possible local circuit with orexin neurons in the LHA.

Early lesion and electronic stimulation studies identified the LHA as an important brain region that regulates multiple processes including feeding, reward behaviors and autonomic function (Bernardis and Bellinger, 1993a). This was further supported at molecular level by the discoveries of LHA specific neuropeptides orexin and MCH which innervate throughout brain and are known to regulate various physiological functions including feeding, sleep/wake cycle, reward behaviors and body energy homeostasis (Berthoud and Munzberg, 2011). A recent study, however, reported that a population of LHA neurons expressing LepRb was completely distinct from orexin and MCH but completely overlapped with

GAD67. These neurons also modulates the midbrain dopamine system to suppress feeding (Leinninger *et al.*, 2009). In the present study, we demonstrate LHA MC4R-positive neurons are a part of this neuronal population and contain anorexigenic peptide NT. Understanding the relevant physiological function of NT release from LHA MC4R/LepR double-positive neurons is of great interest for the future studies.

The interaction of the leptin and melanocortin systems has been extensively investigated and debated. Leptin is a key regulator of POMC expression, the precursor of the melanocortin agonist α-MSH, (Schwartz *et al.*, 1997) and administration of a melanocortin antagonist blocks the anorexigenic effect of leptin administration (Seeley *et al.*, 1997). Additionally, central inhibition of the melanocortin system blunts leptin-induced activation of the sympathetic nervous system and dissipation of excess energy by brown adipose tissue (Dunbar and Lu, 1999; Satoh et al., 1998). In contrast, others have demonstrated that inhibition of both leptin and melanocortin signaling results in additive effect on weight gain and that leptin resistance in melanocortin signaling is a compensatory response to chronic hyperleptinemia (Boston et al., 1997; Trevaskis and Butler, 2005). In addition, deletion of leptin receptors from POMC neurons produces obesity, but is much milder than leptin deficiency suggesting that additional sites are important for leptin action (Balthasar *et al.*, 2004; Hill *et al.*, 2010). Finally, leptin deficient, but not MC4R-null, mice increase thermogenesis and locomotor activity after exposure to HFD (Butler *et al.*, 2001). Our data now identify an overlap of leptin and melanocortin signaling in a small sub-set of neurons in the LHA. This overlap in MC4R and LepRb signaling suggests that this population of neurons may integrate numerous peripheral signals to regulate energy balance.

The degree of cross-talk between MC4R and LepR signaling pathways in this small subset of neurons remains to be elucidated. MC4R signaling has previously been demonstrated *in vitro* to enhance leptin-induced phosphorylation of Stat3 via a MAPK dependent pathway (Zhang *et al.*, 2009b). Interestingly, in this system leptin signaling had no effect on MC4R induced levels of cAMP suggesting that while MC4R modulates LepRb, the converse is not true. Alternatively, we show here that leptin-induced hyperpolarization of LHA neurons is dependent on K_{ATP} channels. A similar mechanism of action occurs in POMC neurons, where leptin and insulin modulate activity of POMC neurons via PI3 kinase-dependent action on K_{ATP} channels (Belgardt et al., 2009; Hill et al., 2008b). Consistent with this model, MC4R signaling has been shown to activate PI3K in transfected CHO-K1 cells (Vongs *et al.*, 2004). Finally, previous work in pancreatic β-cells has demonstrated a role for the cAMP sensor EPAC2 in modulation of K_{ATP} channel activity (Zhang *et al.*, 2009a), suggesting that a similar mechanism might occur in LHA. However recent work has demonstrated that the melanocortin 3/4 receptor agonist MT II was not able to induce EPAC-mediated leptin resistance in hypothalamic POMC neurons (Fukuda *et al.*, 2011).

One area of great interest in the future will be to determine the target of LHA MC4R/NT/LepRb neurons. Previous studies have identified the VTA and DR as regions innervated by LHA LepRb neurons (Leinninger *et al.*, 2009). However, we did not observe any projections of LHA MC4R-GFP neurons to these areas. For other sites we tested, relatively few LHA MC4R-GFP neurons projected to the NTS (<8%) and PBN (<12%) and none projected to the spinal cord. One potential target of MC4R LHA neurons are orexin (also known as hypocretin) expressing neurons in the LHA. These neurons have also been identified as a target of LHA LepRb neurons via a local circuit (Louis *et al.*, 2010b). Consistent with this possibility, we demonstrate here that leptin hyperpolarizes the majority of LHA MC4R-GFP neurons (Fig. 3). Hyperpolarization of the GABAergic neurons would be predicted to disinhibit down stream orexin neurons leading to activation. Indeed, pharmacological administration of either leptin or MT II increases c-Fos expression in orexin neurons at ZT8 (Table 3), although we can not definitely link this effect to LepRb or MC4Rs expressed in

the LHA. Clearly additional neuroanatomical and functional studies will need to be done to delineate the targets of MC4R-LHA neurons. Dissecting this kind of local neuronal circuit will require the development of genetic and trans-synaptic tracing tools, such as a MC4R-Cre mouse line, to directly test the possibility that LHA MC4R-GFP neurons synapse onto local orexin neurons.

Electrophysiological properties of LHA LepR neurons in response to leptin seem to be heterogeneous. Leinninger et al (2009) have shown that leptin depolarizes and hyperpolarizes about 34% and 22% of LHA LepR neurons, respectively, and nearly half of LHA LepR neurons did not respond to leptin. Our electrophysiological recording of LHA MC4R-GFP neurons revealed that leptin hyperpolarizes the majority of neurons we recorded from (10/16) and had no effect on the remaining neurons. Since our double IHC revealed about ~75% of colocalization of LHA MC4R-GFP neurons with LepRb (as determined by pSTAT3), this indicates that leptin hyperpolarizes the majority of LHA MC4R/LepR neurons. It is very interesting that we do not observe a direct depolarization of LHA neurons by a MC4R agonist. This observation suggests the alternative possibility that MC4R signaling may act pre-synaptically at the terminals of LHA MC4R neurons to modulate neurotransmitter release. This has been previously demonstrated for melanocortin receptor expressing neurons in the paraventricular nucleus of the hypothalamus (Cowley *et al.*, 1999) and the nucleus tractus solitarius (Wan *et al.*, 2008). Unfortunately, because orexin neurons within the LHA are a likely target for MC4R-LHA neurons, we cannot distinguish this possibility using pharmacologic techniques. Future studies using genetic methods to specifically manipulate expression of MC4Rs in LHA neurons will need to resolve this question.

In conclusion, we describe a novel population of neurons within the LHA that express both the MC4R and the LepRb. Understanding the function of these neurons may shed important insights into energy homeostasis and the development of obesity.

Acknowledgments

Acknowledgements: This work was also supported by ML (MH084058-01A1, Disease Oriented Clinical Scholar Award and NARSAD Young Investigator Award), KWW (K01DK087780) and JKE (R01DK53301 and RL1DK081185).

Other Acknowledgements: We thank Jeffrey Friedman for use of MC4R-GFP mice and Carol F. Elias and Yuichi Sato for technical assistance.

Literature Cited

Al-Khater KM, Kerr R, Todd AJ. A quantitative study of spinothalamic neurons in laminae I, III, and IV in lumbar and cervical segments of the rat spinal cord. J Comp Neurol. 2008; 511(1):1–18. [PubMed: 18720412]

Bagnol D, Lu XY, Kaelin CB, Day HE, Ollmann M, Gantz I, Akil H, Barsh GS, Watson SJ. Anatomy of an endogenous antagonist: relationship between Agouti-related protein and proopiomelanocortin in brain. J Neurosci. 1999; 19(18):RC26. [PubMed: 10479719]

Balthasar N, Coppari R, McMinn J, Liu SM, Lee CE, Tang V, Kenny CD, McGovern RA, Chua SC Jr, Elmquist JK, Lowell BB. Leptin receptor signaling in POMC neurons is required for normal body weight homeostasis. Neuron. 2004; 42(6):983–991. [PubMed: 15207242]

Balthasar N, Dalgaard LT, Lee CE, Yu J, Funahashi H, Williams T, Ferreira M, Tang V, McGovern RA, Kenny CD, Christiansen LM, Edelstein E, Choi B, Boss O, Aschkenasi C, Zhang CY, Mountjoy K, Kishi T, Elmquist JK, Lowell BB. Divergence of melanocortin pathways in the control of food intake and energy expenditure. Cell. 2005; 123(3):493–505. [PubMed: 16269339]

Belgardt BF, Okamura T, Bruning JC. Hormone and glucose signalling in POMC and AgRP neurons. J Physiol. 2009; 587(Pt 22):5305–5314. [PubMed: 19770186]

Benoit SC, Schwartz MW, Lachey JL, Hagan MM, Rushing PA, Blake KA, Yagaloff KA, Kurylko G, Franco L, Danhoo W, Seeley RJ. A novel selective melanocortin-4 receptor agonist reduces food intake in rats and mice without producing aversive consequences. J Neurosci. 2000; 20(9):3442–3448. [PubMed: 10777807]

Berman JR, Skariah G, Maro GS, Mignot E, Mourrain P. Characterization of two melanin-concentrating hormone genes in zebrafish reveals evolutionary and physiological links with the mammalian MCH system. J Comp Neurol. 2009; 517(5):695–710. [PubMed: 19827161]

Bernardis LL, Bellinger LL. The lateral hypothalamic area revisited: neuroanatomy, body weight regulation, neuroendocrinology and metabolism. Neuroscience and biobehavioral reviews. 1993a; 17(2):141–193. [PubMed: 8515901]

Bernardis LL, Bellinger LL. The lateral hypothalamic area revisited: neuroanatomy, body weight regulation, neuroendocrinology and metabolism. Neurosci Biobehav Rev. 1993b; 17(2):141–193. [PubMed: 8515901]

Berthoud HR, Munzberg H. The lateral hypothalamus as integrator of metabolic and environmental needs: From electrical self-stimulation to opto-genetics. Physiology & behavior. 2011; 104(1):29–39. [PubMed: 21549732]

Bjorbaek C, Hollenberg AN. Leptin and melanocortin signaling in the hypothalamus. Vitam Horm. 2002; 65:281–311. [PubMed: 12481551]

Boston BA, Blaydon KM, Varnerin J, Cone RD. Independent and additive effects of central POMC and leptin pathways on murine obesity. Science. 1997; 278(5343):1641–1644. [PubMed: 9374468]

Brailoiu GC, Dun SL, Brailoiu E, Inan S, Yang J, Chang JK, Dun NJ. Nesfatin-1: distribution and interaction with a G protein-coupled receptor in the rat brain. Endocrinology. 2007; 148(10):5088–5094. [PubMed: 17627999]

Bulloch K, Miller MM, Gal-Toth J, Milner TA, Gottfried-Blackmore A, Waters EM, Kaunzner UW, Liu K, Lindquist R, Nussenzweig MC, Steinman RM, McEwen BS. CD11c/EYFP transgene illuminates a discrete network of dendritic cells within the embryonic, neonatal, adult, and injured mouse brain. J Comp Neurol. 2008; 508(5):687–710. [PubMed: 18386786]

Butler AA, Marks DL, Fan W, Kuhn CM, Bartolome M, Cone RD. Melanocortin-4 receptor is required for acute homeostatic responses to increased dietary fat. Nat Neurosci. 2001; 4(6):605–611. [PubMed: 11369941]

Chamberlin NL, Du B, de Lacalle S, Saper CB. Recombinant adeno-associated virus vector: use for transgene expression and anterograde tract tracing in the CNS. Brain Res. 1998; 793(1–2):169–175. [PubMed: 9630611]

Chen AS, Metzger JM, Trumbauer ME, Guan XM, Yu H, Frazier EG, Marsh DJ, Forrest MJ, Gopal-Truter S, Fisher J, Camacho RE, Strack AM, Mellin TN, MacIntyre DE, Chen HY, Van der Ploeg LH. Role of the melanocortin-4 receptor in metabolic rate and food intake in mice. Transgenic Res. 2000; 9(2):145–154. [PubMed: 10951699]

Cone RD. Anatomy and regulation of the central melanocortin system. Nat Neurosci. 2005; 8(5):571–578. [PubMed: 15856065]

Cone RD. Studies on the physiological functions of the melanocortin system. Endocrine reviews. 2006; 27(7):736–749. [PubMed: 17077189]

Cowley MA, Pronchuk N, Fan W, Dinulescu DM, Colmers WF, Cone RD. Integration of NPY, AGRP, and melanocortin signals in the hypothalamic paraventricular nucleus: evidence of a cellular basis for the adipostat. Neuron. 1999; 24(1):155–163. [PubMed: 10677034]

Cui H, Cai F, Belsham DD. Anorexigenic hormones leptin, insulin, and alpha-melanocyte-stimulating hormone directly induce neurotensin (NT) gene expression in novel NT-expressing cell models. J Neurosci. 2005; 25(41):9497–9506. [PubMed: 16221860]

Dunbar JC, Lu H. Leptin-induced increase in sympathetic nervous and cardiovascular tone is mediated by proopiomelanocortin (POMC) products. Brain Res Bull. 1999; 50(3):215–221. [PubMed: 10566984]

Elias CF, Aschkenasi C, Lee C, Kelly J, Ahima RS, Bjorbaek C, Flier JS, Saper CB, Elmquist JK. Leptin differentially regulates NPY and POMC neurons projecting to the lateral hypothalamic area. Neuron. 1999; 23(4):775–786. [PubMed: 10482243]

Elmquist JK, Elias CF, Saper CB. From lesions to leptin: hypothalamic control of food intake and body weight. Neuron. 1999; 22(2):221–232. [PubMed: 10069329]

Estabrooke IV, McCarthy MT, Ko E, Chou TC, Chemelli RM, Yanagisawa M, Saper CB, Scammell TE. Fos expression in orexin neurons varies with behavioral state. J Neurosci. 2001; 21(5):1656–1662. [PubMed: 11222656]

Fan W, Boston BA, Kesterson RA, Hruby VJ, Cone RD. Role of melanocortinergic neurons in feeding and the agouti obesity syndrome. Nature. 1997; 385(6612):165–168. [PubMed: 8990120]

Florenzano F, Viscomi MT, Mercaldo V, Longone P, Bernardi G, Bagni C, Molinari M, Carrive P. P2X2R purinergic receptor subunit mRNA and protein are expressed by all hypothalamic hypocretin/orexin neurons. J Comp Neurol. 2006; 498(1):58–67. [PubMed: 16856176]

Fukuda M, Williams KW, Gautron L, Elmquist JK. Induction of leptin resistance by activation of cAMP-Epac signaling. Cell Metab. 2011; 13(3):331–339. [PubMed: 21356522]

Funato H, Tsai AL, Willie JT, Kisanuki Y, Williams SC, Sakurai T, Yanagisawa M. Enhanced orexin receptor-2 signaling prevents diet-induced obesity and improves leptin sensitivity. Cell Metab. 2009; 9(1):64–76. [PubMed: 19117547]

Garcia-Galiano D, Navarro VM, Gaytan F, Tena-Sempere M. Expanding roles of NUCB2/nesfatin-1 in neuroendocrine regulation. J Mol Endocrinol. 2010; 45(5):281–290. [PubMed: 20682642]

Gautron L, Lazarus M, Scott MM, Saper CB, Elmquist JK. Identifying the efferent projections of leptin-responsive neurons in the dorsomedial hypothalamus using a novel conditional tracing approach. J Comp Neurol. 2010a; 518(11):2090–2108. [PubMed: 20394060]

Gautron L, Lee C, Funahashi H, Friedman J, Lee S, Elmquist J. Melanocortin-4 receptor expression in a vago-vagal circuitry involved in postprandial functions. J Comp Neurol. 2010b; 518(1):6–24. [PubMed: 19882715]

Geisler S, Zahm DS. On the retention of neurotensin in the ventral tegmental area (VTA) despite destruction of the main neurotensinergic afferents of the VTA--implications for the organization of forebrain projections to the VTA. Brain Res. 2006; 1087(1):87–104. [PubMed: 16626637]

Ghamari-Langroudi M, Srisai D, Cone RD. Multinodal regulation of the arcuate/paraventricular nucleus circuit by leptin. Proc Natl Acad Sci U S A. 2011; 108(1):355–360. [PubMed: 21169216]

Glavas MM, Grayson BE, Allen SE, Copp DR, Smith MS, Cowley MA, Grove KL. Characterization of brainstem peptide YY (PYY) neurons. J Comp Neurol. 2008; 506(2):194–210. [PubMed: 18022952]

Haring JH, Davis JN. Acetylcholinesterase neurons in the lateral hypothalamus project to the spinal cord. Brain Res. 1983; 268(2):275–283. [PubMed: 6191833]

Harris M, Aschkenasi C, Elias CF, Chandrankunnel A, Nillni EA, Bjoorbaek C, Elmquist JK, Flier JS, Hollenberg AN. Transcriptional regulation of the thyrotropin-releasing hormone gene by leptin and melanocortin signaling. J Clin Invest. 2001; 107(1):111–120. [PubMed: 11134186]

Harrison SJ, Parrish M, Monaghan AP. Sall3 is required for the terminal maturation of olfactory glomerular interneurons. J Comp Neurol. 2008; 507(5):1780–1794. [PubMed: 18260139]

Hill JW, Elias CF, Fukuda M, Williams KW, Berglund ED, Holland WL, Cho YR, Chuang JC, Xu Y, Choi M, Lauzon D, Lee CE, Coppari R, Richardson JA, Zigman JM, Chua S, Scherer PE, Lowell BB, Bruning JC, Elmquist JK. Direct insulin and leptin action on proopiomelanocortin neurons is required for normal glucose homeostasis and fertility. Cell Metab. 2010; 11(4):286–297. [PubMed: 20374961]

Hill JW, Williams KW, Ye C, Luo J, Balthasar N, Coppari R, Cowley MA, Cantley LC, Lowell BB, Elmquist JK. Acute effects of leptin require PI3K signaling in hypothalamic proopiomelanocortin neurons in mice. J Clin Invest. 2008a; 118(5):1796–1805. [PubMed: 18382766]

Hill JW, Williams KW, Ye C, Luo J, Balthasar N, Coppari R, Cowley MA, Cantley LC, Lowell BB, Elmquist JK. Acute effects of leptin require PI3K signaling in hypothalamic proopiomelanocortin neurons in mice. J Clin Invest. 2008b; 118(5):1796–1805. [PubMed: 18382766]

Howorth PW, Teschemacher AG, Pickering AE. Retrograde adenoviral vector targeting of nociresponsive pontospinal noradrenergic neurons in the rat in vivo. J Comp Neurol. 2009; 512(2):141–157. [PubMed: 19003793]

Kaczmarek L, Nikolajew E. c-fos protooncogene expression and neuronal plasticity. Acta Neurobiol Exp (Wars). 1990; 50(4–5):173–179. [PubMed: 2130639]

Kas MJ, Tiesjema B, van Dijk G, Garner KM, Barsh GS, ter Brake O, Verhaagen J, Adan RA. Induction of brain-region-specific forms of obesity by agouti. J Neurosci. 2004; 24(45):10176–10181. [PubMed: 15537888]

Kelley AE, Baldo BA, Pratt WE. A proposed hypothalamic-thalamic-striatal axis for the integration of energy balance, arousal, and food reward. J Comp Neurol. 2005; 493(1):72–85. [PubMed: 16255002]

Kelly AB, Watts AG. The region of the pontine parabrachial nucleus is a major target of dehydration-sensitive CRH neurons in the rat lateral hypothalamic area. J Comp Neurol. 1998; 394(1):48–63. [PubMed: 9550142]

Kim MS, Rossi M, Abusnana S, Sunter D, Morgan DG, Small CJ, Edwards CM, Heath MM, Stanley SA, Seal LJ, Bhatti JR, Smith DM, Ghatei MA, Bloom SR. Hypothalamic localization of the feeding effect of agouti-related peptide and alpha-melanocyte-stimulating hormone. Diabetes. 2000; 49(2):177–182. [PubMed: 10868932]

Kishi T, Aschkenasi CJ, Lee CE, Mountjoy KG, Saper CB, Elmquist JK. Expression of melanocortin 4 receptor mRNA in the central nervous system of the rat. Journal of Comparative Neurology. 2003; 457(3):213–235. [PubMed: 12541307]

Kishi T, Tsumori T, Ono K, Yokota S, Ishino H, Yasui Y. Topographical organization of projections from the subiculum to the hypothalamus in the rat. J Comp Neurol. 2000; 419(2):205–222. [PubMed: 10722999]

Kohno D, Nakata M, Maejima Y, Shimizu H, Sedbazar U, Yoshida N, Dezaki K, Onaka T, Mori M, Yada T. Nesfatin-1 neurons in paraventricular and supraoptic nuclei of the rat hypothalamus coexpress oxytocin and vasopressin and are activated by refeeding. Endocrinology. 2008; 149(3): 1295–1301. [PubMed: 18048495]

Lefler Y, Arzi A, Reiner K, Sukhotinsky I, Devor M. Bulbospinal neurons of the rat rostromedial medulla are highly collateralized. J Comp Neurol. 2008; 506(6):960–978. [PubMed: 18085592]

Leinninger GM, Jo YH, Leshan RL, Louis GW, Yang H, Barrera JG, Wilson H, Opland DM, Faouzi MA, Gong Y, Jones JC, Rhodes CJ, Chua S Jr, Diano S, Horvath TL, Seeley RJ, Becker JB, Munzberg H, Myers MG Jr. Leptin acts via leptin receptor-expressing lateral hypothalamic neurons to modulate the mesolimbic dopamine system and suppress feeding. Cell Metab. 2009; 10(2):89–98. [PubMed: 19656487]

Leinninger GM, Opland DM, Jo YH, Faouzi M, Christensen L, Cappellucci LA, Rhodes CJ, Gnegy ME, Becker JB, Pothos EN, Seasholtz AF, Thompson RC, Myers MGJ. Leptin action via neurotensin neurons controls orexin, the mesolimbic dopamine system and energy balance. Cell Metab. 2011; 14(3):313–323. [PubMed: 21907138]

Li J, Xiong K, Pang Y, Dong Y, Kaneko T, Mizuno N. Medullary dorsal horn neurons providing axons to both the parabrachial nucleus and thalamus. J Comp Neurol. 2006; 498(4):539–551. [PubMed: 16874804]

Liu H, Kishi T, Roseberry AG, Cai X, Lee CE, Montez JM, Friedman JM, Elmquist JK. Transgenic mice expressing green fluorescent protein under the control of the melanocortin-4 receptor promoter. Journal of Neuroscience. 2003; 23(18):7143–7154. [PubMed: 12904474]

Liu M, Thankachan S, Kaur S, Begum S, Blanco-Centurion C, Sakurai T, Yanagisawa M, Neve R, Shiromani PJ. Orexin (hypocretin) gene transfer diminishes narcoleptic sleep behavior in mice. Eur J Neurosci. 2008; 28(7):1382–1393. [PubMed: 18973565]

Liu X, Zeng J, Zhou A, Theodorsson E, Fahrenkrug J, Reinscheid RK. Molecular fingerprint of neuropeptide S-producing neurons in the mouse brain. J Comp Neurol. 2011; 519(10):1847–1866. [PubMed: 21452230]

Louis GW, Leinninger GM, Rhodes CJ, Myers MG Jr. Direct innervation and modulation of orexin neurons by lateral hypothalamic LepRb neurons. J Neurosci. 2010a; 30(34):11278–11287. [PubMed: 20739548]

Louis GW, Leinninger GM, Rhodes CJ, Myers MG Jr. Direct Innervation and Modulation of Orexin Neurons by Lateral Hypothalamic LepRb Neurons. Journal of Neuroscience. 2010b; 30(34): 11278–11287. [PubMed: 20739548]

Lu XY, Barsh GS, Akil H, Watson SJ. Interaction between alpha-melanocyte-stimulating hormone and corticotropin-releasing hormone in the regulation of feeding and hypothalamo-pituitary-adrenal responses. J Neurosci. 2003; 23(21):7863–7872. [PubMed: 12944516]

Marsh DJ, Hollopeter G, Huszar D, Laufer R, Yagaloff KA, Fisher SL, Burn P, Palmiter RD. Response of melanocortin-4 receptor-deficient mice to anorectic and orexigenic peptides. Nat Genet. 1999; 21(1):119–122. [PubMed: 9916804]

Moga MM, Saper CB, Gray TS. Neuropeptide organization of the hypothalamic projection to the parabrachial nucleus in the rat. J Comp Neurol. 1990; 295(4):662–682. [PubMed: 1972710]

Moore RY, Speh JC, Leak RK. Suprachiasmatic nucleus organization. Cell Tissue Res. 2002; 309(1): 89–98. [PubMed: 12111539]

Mountjoy KG, Mortrud MT, Low MJ, Simerly RB, Cone RD. Localization of the melanocortin-4 receptor (MC4-R) in neuroendocrine and autonomic control circuits in the brain. Mol Endocrinol. 1994; 8(10):1298–1308. [PubMed: 7854347]

Oh IS, Shimizu H, Satoh T, Okada S, Adachi S, Inoue K, Eguchi H, Yamamoto M, Imaki T, Hashimoto K, Tsuchiya T, Monden T, Horiguchi K, Yamada M, Mori M. Identification of nesfatin-1 as a satiety molecule in the hypothalamus. Nature. 2006; 443(7112):709–712. [PubMed: 17036007]

Reznikov LR, Reagan LP, Fadel JR. Activation of phenotypically distinct neuronal subpopulations in the anterior subdivision of the rat basolateral amygdala following acute and repeated stress. J Comp Neurol. 2008; 508(3):458–472. [PubMed: 18335544]

Santini F, Maffei M, Pelosini C, Salvetti G, Scartabelli G, Pinchera A. Melanocortin-4 receptor mutations in obesity. Adv Clin Chem. 2009; 48:95–109. [PubMed: 19803416]

Saper CB, Chou TC, Elmquist JK. The need to feed: homeostatic and hedonic control of eating. Neuron. 2002; 36(2):199–211. [PubMed: 12383777]

Satoh N, Ogawa Y, Katsuura G, Numata Y, Masuzaki H, Yoshimasa Y, Nakao K. Satiety effect and sympathetic activation of leptin are mediated by hypothalamic melanocortin system. Neurosci Lett. 1998; 249(2–3):107–110. [PubMed: 9682828]

Schwartz MW, Seeley RJ, Woods SC, Weigle DS, Campfield LA, Burn P, Baskin DG. Leptin increases hypothalamic pro-opiomelanocortin mRNA expression in the rostral arcuate nucleus. Diabetes. 1997; 46(12):2119–2123. [PubMed: 9392508]

Schwartz MW, Woods SC, Porte D Jr, Seeley RJ, Baskin DG. Central nervous system control of food intake. Nature. 2000; 404(6778):661–671. [PubMed: 10766253]

Scott MM, Lachey JL, Sternson SM, Lee CE, Elias CF, Friedman JM, Elmquist JK. Leptin targets in the mouse brain. J Comp Neurol. 2009; 514(5):518–532. [PubMed: 19350671]

Seeley RJ, Yagaloff KA, Fisher SL, Burn P, Thiele TE, van Dijk G, Baskin DG, Schwartz MW. Melanocortin receptors in leptin effects. Nature. 1997; 390(6658):349. [PubMed: 9389472]

Shimizu H, Inoue K, Mori M. The leptin-dependent and -independent melanocortin signaling system: regulation of feeding and energy expenditure. Journal of Endocrinology. 2007; 193(1):1–9. [PubMed: 17400797]

Shin JW, Geerling JC, Loewy AD. Inputs to the ventrolateral bed nucleus of the stria terminalis. J Comp Neurol. 2008; 511(5):628–657. [PubMed: 18853414]

Shroyer NF, Wallis D, Venken KJ, Bellen HJ, Zoghbi HY. Gfi1 functions downstream of Math1 to control intestinal secretory cell subtype allocation and differentiation. Genes Dev. 2005; 19(20): 2412–2417. [PubMed: 16230531]

Srisai D, Gillum MP, Panaro BL, Zhang XM, Kotchabhakdi N, Shulman GI, Ellacott KL, Cone RD. Characterization of the hyperphagic response to dietary fat in the MC4R knockout mouse. Endocrinology. 2011; 152(3):890–902. [PubMed: 21239438]

Tokita K, Inoue T, Boughter JD Jr. Afferent connections of the parabrachial nucleus in C57BL/6J mice. Neuroscience. 2009; 161(2):475–488. [PubMed: 19327389]

Trevaskis JL, Butler AA. Double leptin and melanocortin-4 receptor gene mutations have an additive effect on fat mass and are associated with reduced effects of leptin on weight loss and food intake. Endocrinology. 2005; 146(10):4257–4265. [PubMed: 15994342]

Vongs A, Lynn NM, Rosenblum CI. Activation of MAP kinase by MC4-R through PI3 kinase. Regul Pept. 2004; 120(1–3):113–118. [PubMed: 15177928]

Wan S, Browning KN, Coleman FH, Sutton G, Zheng H, Butler A, Berthoud HR, Travagli RA. Presynaptic melanocortin-4 receptors on vagal afferent fibers modulate the excitability of rat nucleus tractus solitarius neurons. J Neurosci. 2008; 28(19):4957–4966. [PubMed: 18463249]

WHO. Report of a WHO Consultation. second ed.. Geneva, Switzerland: World Health Organization; 2004. Obesity: Preventing and Managing the Global Epidemic; p. 253

Williams KW, Margatho LO, Lee CE, Choi M, Lee S, Scott MM, Elias CF, Elmquist JK. Segregation of acute leptin and insulin effects in distinct populations of arcuate proopiomelanocortin neurons. J Neurosci. 2010; 30(7):2472–2479. [PubMed: 20164331]

Wittmann G, Fuzesi T, Singru PS, Liposits Z, Lechan RM, Fekete C. Efferent projections of thyrotropin-releasing hormone-synthesizing neurons residing in the anterior parvocellular subdivision of the hypothalamic paraventricular nucleus. J Comp Neurol. 2009; 515(3):313–330. [PubMed: 19425088]

Xu X, Roby KD, Callaway EM. Immunochemical characterization of inhibitory mouse cortical neurons: three chemically distinct classes of inhibitory cells. J Comp Neurol. 2010; 518(3):389–404. [PubMed: 19950390]

Yee CL, Wang Y, Anderson S, Ekker M, Rubenstein JL. Arcuate nucleus expression of NKX2.1 and DLX and lineages expressing these transcription factors in neuropeptide Y(+), proopiomelanocortin(+), and tyrosine hydroxylase(+) neurons in neonatal and adult mice. J Comp Neurol. 2009; 517(1):37–50. [PubMed: 19711380]

Zahm DS, Cheng AY, Lee TJ, Ghobadi CW, Schwartz ZM, Geisler S, Parsely KP, Gruber C, Veh RW. Inputs to the midbrain dopaminergic complex in the rat, with emphasis on extended amygdala-recipient sectors. J Comp Neurol. 2011; 519(16):3159–3188. [PubMed: 21618227]

Zhang CL, Katoh M, Shibasaki T, Minami K, Sunaga Y, Takahashi H, Yokoi N, Iwasaki M, Miki T, Seino S. The cAMP sensor Epac2 is a direct target of antidiabetic sulfonylurea drugs. Science. 2009a; 325(5940):607–610. [PubMed: 19644119]

Zhang Y, Proenca R, Maffei M, Barone M, Leopold L, Friedman JM. Positional cloning of the mouse obese gene and its human homologue. Nature. 1994; 372(6505):425–432. [PubMed: 7984236]

Zhang Y, Wu X, He Y, Kastin AJ, Hsuchou H, Rosenblum CI, Pan W. Melanocortin potentiates leptin-induced STAT3 signaling via MAPK pathway. J Neurochem. 2009b; 110(1):390–399. [PubMed: 19457101]

Zhao Y, Flandin P, Long JE, Cuesta MD, Westphal H, Rubenstein JL. Distinct molecular pathways for development of telencephalic interneuron subtypes revealed through analysis of Lhx6 mutants. J Comp Neurol. 2008; 510(1):79–99. [PubMed: 18613121]

Zheng H, Patterson LM, Berthoud HR. Orexin-A projections to the caudal medulla and orexin-induced c-Fos expression, food intake, and autonomic function. J Comp Neurol. 2005; 485(2):127–142. [PubMed: 15776447]

Zheng H, Patterson LM, Berthoud HR. Orexin signaling in the ventral tegmental area is required for high-fat appetite induced by opioid stimulation of the nucleus accumbens. J Neurosci. 2007; 27(41):11075–11082. [PubMed: 17928449]

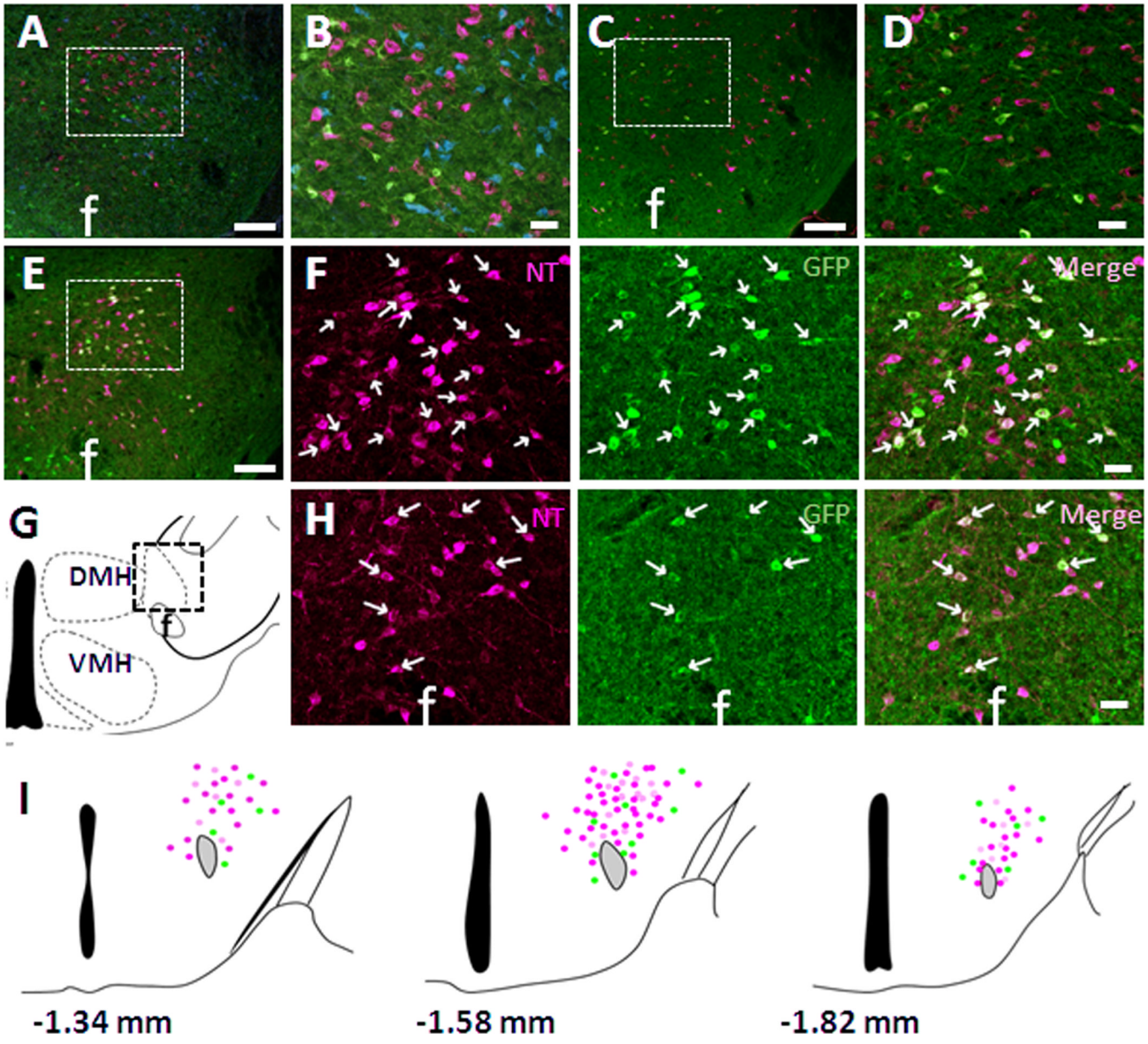

Figure 1. Neurochemical phenotype of LHA MC4R-GFP neurons

Multiple fluorescent IHC in colchicine-treated MC4R-GFP mouse brain sections revealed that LHA MC4R-GFP neurons (green) were completely distinct from orexin (A, B, magenta), MCH (A, B, blue) and nesfatin-1 (C, D, magenta) but colocalized with NT (magenta) in both dorsal LHA (E, F) and perifornical area (G, H). B and D are digital zoom of boxed regions of A and B, respectively. F is digital zoom of boxed region of E shown by individual fluorescent signal channels. (I) Schematic drawing of distribution of NT (magenta), MC4R-GFP (green) and double-positive (white) cells in 3 different levels of the LHA. Note that actual expression of NT and MC4R-GFP cells in other hypothalamic nuclei is not presented here. f, fornix; DMH, dorsomedial hypothalamus; VMH, ventromedial hypothalamus. White arrows indicate representative colocalization. Scale bars: A, B, C, 120 *um*; A', B', C', D', 60 *um*.

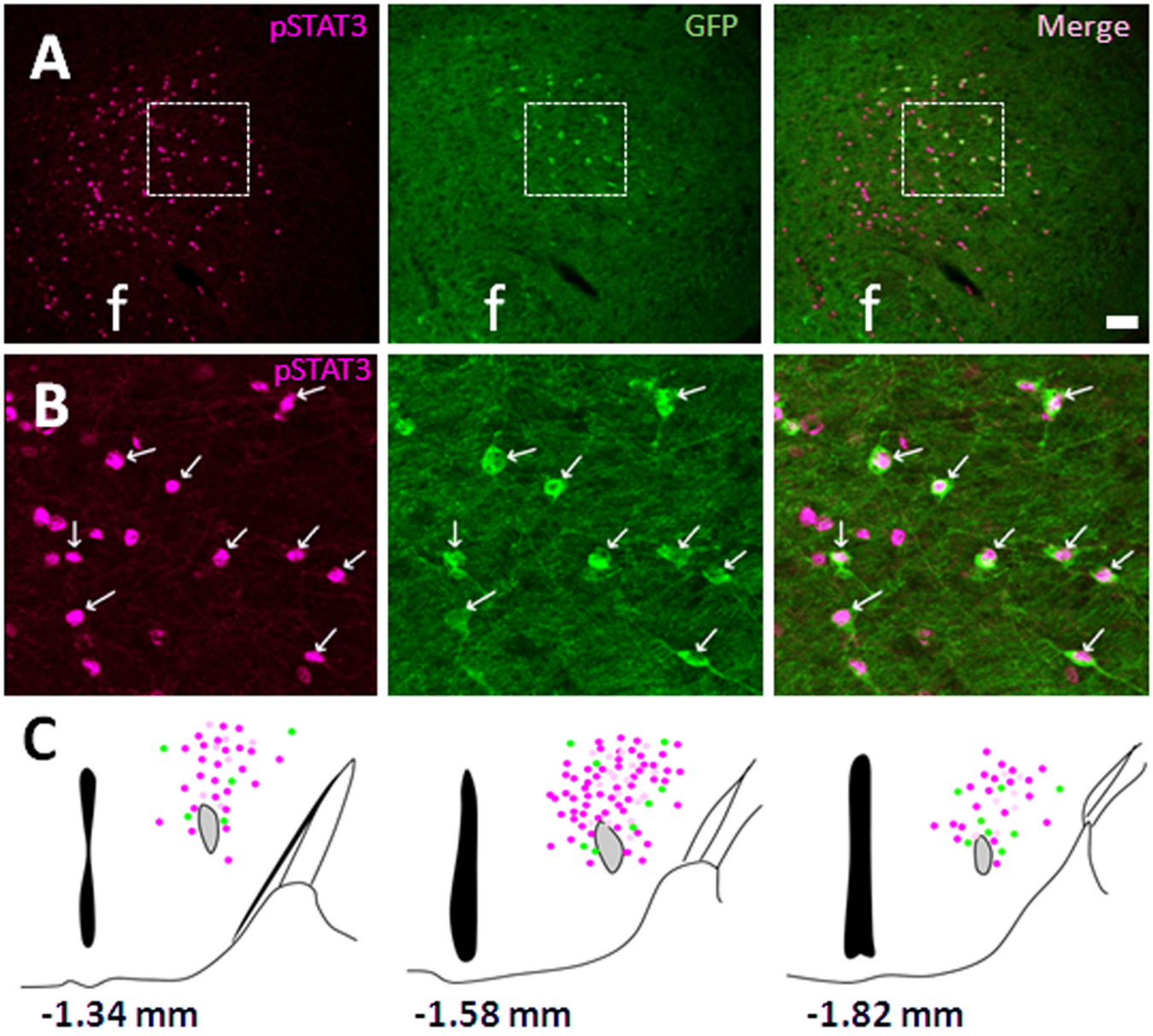

Figure 2. Co-localization of MC4R-GFP neurons with leptin-induced pSTAT3

Double fluorescent IHC in ICV leptin-treated MC4R-GFP mouse brain sections revealed that leptin-induced pSTAT3 (magenta) and MC4R-GFP (green) are co-expressed in the mid-dorsal LHA (A). Digital zoom of boxed region in (A) is showed in (B). (C) Schematic drawing of distribution of pSTAT3 (magenta), MC4R-GFP (green) and double-positive (white) cells in 3 different levels of the LHA. Note that actual expression of NT and MC4R-GFP cells in other hypothalamic nuclei is not presented here. White arrows indicate representative co-localization. f, fornix; Scale bars: A, 80 *um*; B, 40 *um*.

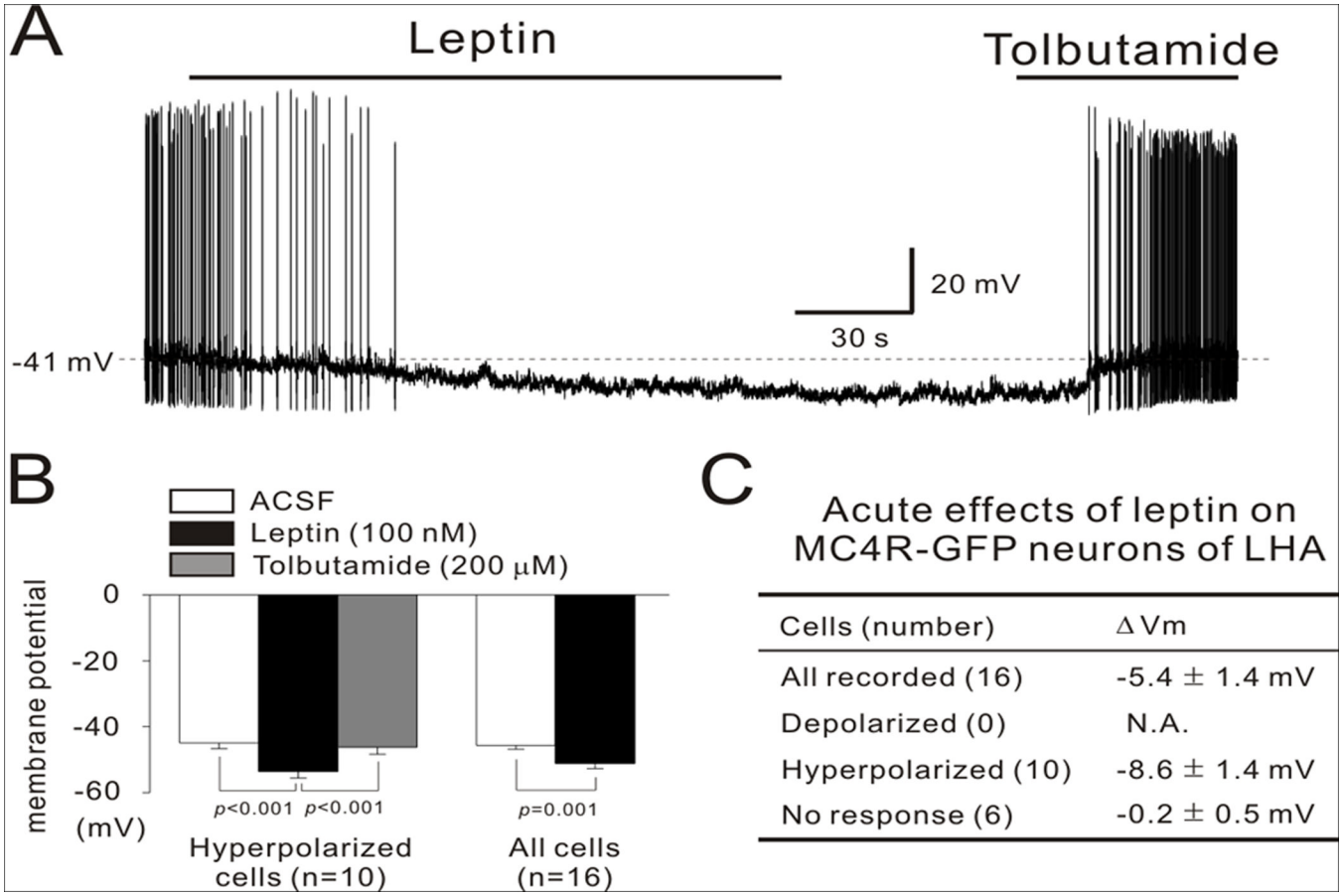

Figure 3. Leptin hyperpolarizes LHA MC4R-GFP neurons via KATP channels

(A) Representative figure showing that bath application of leptin (100 nM) hyperpolarized the membrane potential of LHA MC4R-GFP neurons, which was completely reversed by the KATP channel blocker tolbutamide (200 uM). (B) In the hyperpolarized cell group, the average membrane potential (−44.9 ± 1.7 mV) was significantly hyperpolarized by leptin (−53.5 ± 2.0 mV) in 10 cells. This hyperpolarization was completely recovered by tolbutamide (−46.2 ± 2.2 mV). Leptin also had a significant hyperpolarizing effect on the average membrane potential of all recorded cells (from −45.7 ± 1.2 mV to −51.1 ± 1.6 mV in 16 cells). (C) This table summarizes the acute responses of MC4R-GFP neurons in the LHA to leptin. (D) Representative figure showing that bath application of MC4R agonist MTII had no effect on membrane potential of LHA MC4R-GFP neurons. Data are presented as mean ± S.E.M.

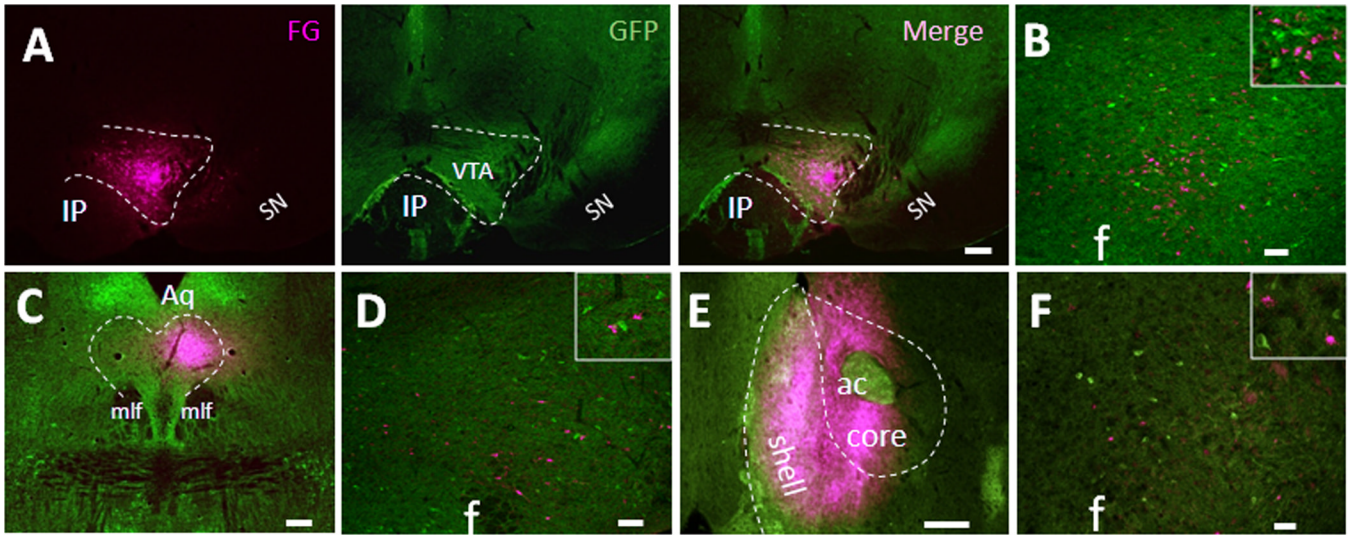

Figure 4. LHA MC4R-GFP neurons do not project to the ventral tegmental area, dorsal raphe and nucleus accumbens

Retrograde neuronal tracers were injected into the VTA, DR and NAc of MC4R-GFP mice and 5~7 days post-surgery, mice were perfused with 4% PFA and brain sections were processed for double fluorescent IHC for GFP and tracer. (A) Representative precise injection site of the VTA was shown by individual fluorescent channels. (B). Representative LHA double fluorescent IHC image from precise VTA-injected cases with retrograde tracer (magenta) and MC4R-GFP (green). Boxed region is digital zoom of the image. (C) Representative precise injection site of the DR. (D). Representative LHA double fluorescent IHC image from precise DR-injected cases with retrograde tracer (magenta) and MC4R-GFP (green). Boxed region is digital zoom of the image. (E) Representative precise injection site of the Nac. (F). Representative LHA double fluorescent IHC image from precise NAc-injected cases with retrograde tracer (magenta) and MC4R-GFP (green). Boxed region is digital zoom of the image. IP, interpeduncular nucleus; SN, substantia nigra; Aq, Aquaduct; mlf, medial longitudinal fasciculus; ac, anterior commissure; f, fornix. Scale bars: A and C, 240 *um*; B, D and F, 80 *um;* E, *320 um*.

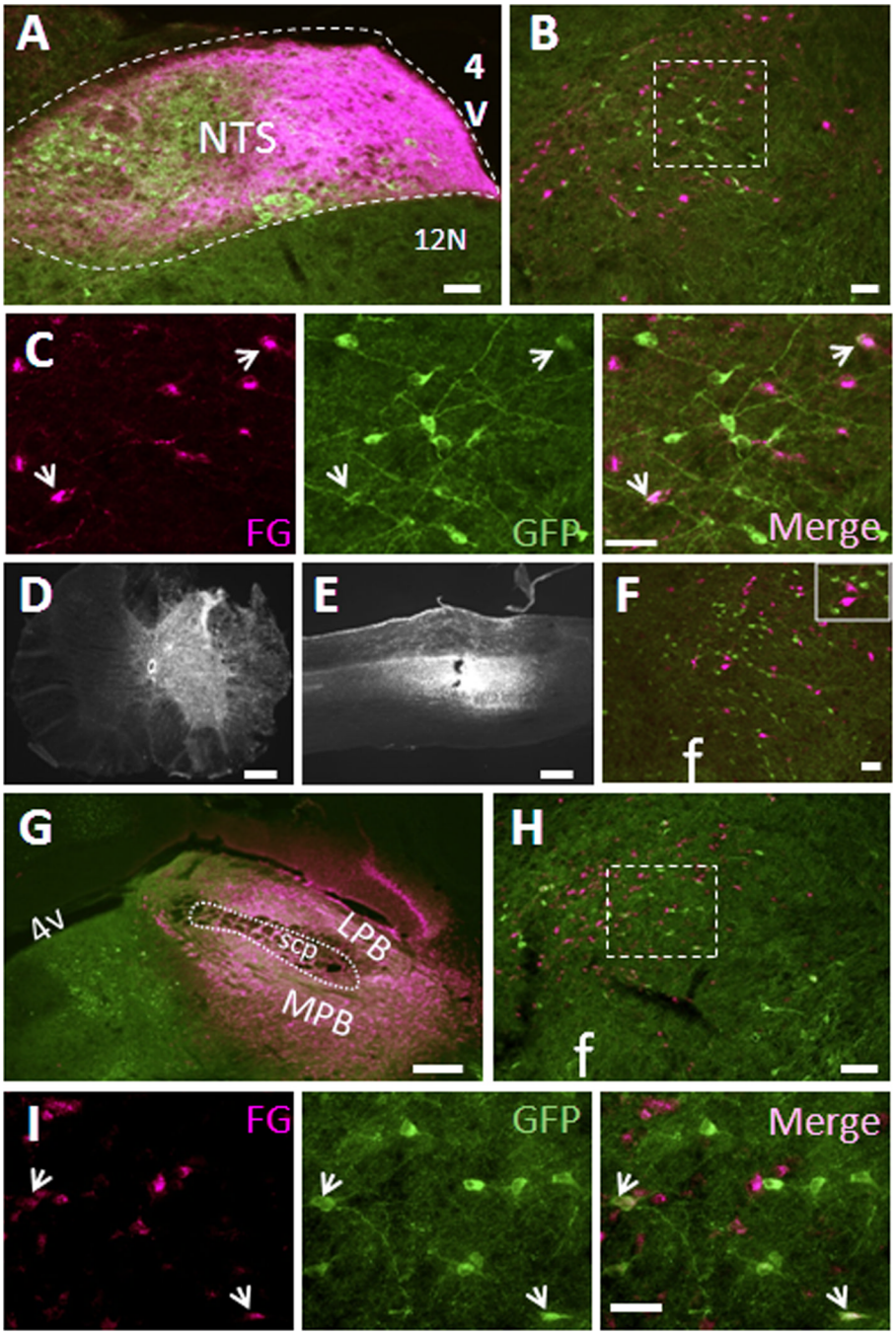

Figure 5. Limited numbers of LHA MC4R-GFP neurons project to the nucleus of solitary tract and the parabrachial nucleus but not spinal cord

Retrograde neuronal tracers were injected into the NTS, PBN and spinal cord of MC4R-GFP mice and 5~7 days post-surgery, mice were perfused with 4% PFA and brain sections were processed for double fluorescent IHC for GFP (green) and tracer (red). (A) Representative precise injection site of the NTS. (B). Representative LHA double fluorescent IHC image from precise NTS-injected cases with retrograde tracer (magenta) and MC4R-GFP (green). (C) Digital zoom of boxed region in (B) was shown by individual fluorescent channels. White arrows indicate colocalization. (D and E) Correct injection site of spinal cord was shown by coronal and sagittal sections, respectively. (F) Representative LHA double

fluorescent IHC image from spinal cord-injected cases with retrograde tracer (magenta) and MC4R-GFP (green). Boxed region is digital zoom of the image. (G) Representative precise injection site of the PBN. (H). Representative LHA double fluorescent IHC image from precise PBN-injected cases with retrograde tracer (magenta) and MC4R-GFP (green). (I) Digital zoom of boxed region in (H) was shown by individual fluorescent channels. White arrows indicate colocalization. NTS, nucleus of solitary tract; 12N, hypoglossal nucleus; scp, superior cerebellar peduncle; LPB, lateral parabrachial nucleus; MPB, medial parabrachial nucleus; 4V, fourth ventricle; f, fornix. Scale bars: A, B, F and H, 80 *um; C* and I, 40 um; D, E and G, 320 *um*.

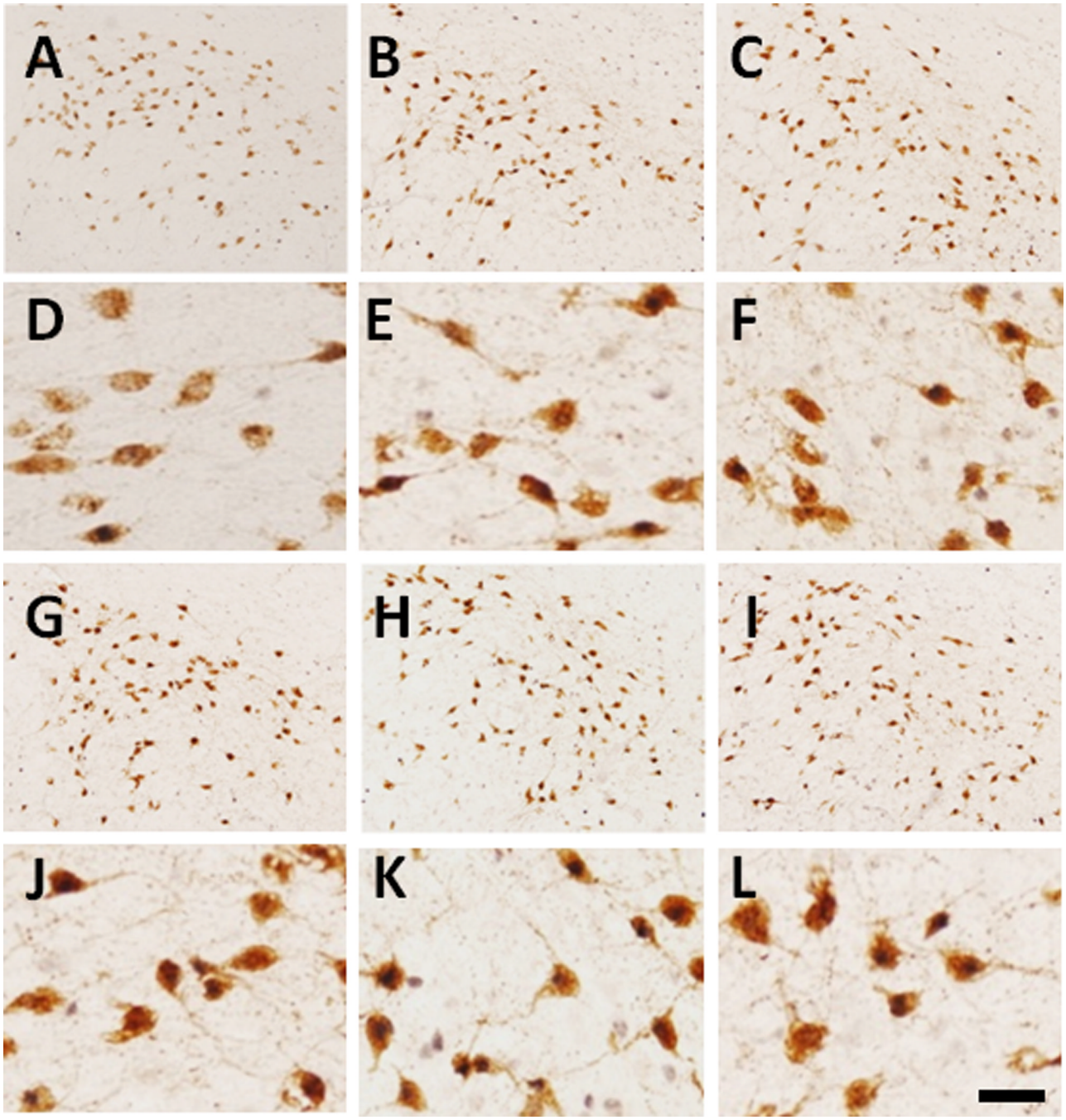

Figure 6. MTII- and leptin-induced c-Fos on orexin neurons

Representative images showing c-Fos expression (dark brown nuclei) within orexin neurons (brown soma) by saline, MTII and leptin. A–C, Mice received saline (A), MTII (B) and leptin (C) at ZT6 and killed 2 hours later (ZT8). D, E and F are digital zoom in of A, B and C, respectively. G–I, Mice received saline (G), MTII (H) and leptin (I) at ZT18 and killed 2 hours latter (ZT20). J, K and L are digital zoom in of G, H and I, respectively. Scale bar: 80 *um.*

Table 1

Primary antibodies used in present study

Antigen	Immunogen	Manufacturer	Dilution used
GFP	Purified recombinant GFP emulsified in Freund's adjuvant	Aves Labs (Tigard, OR), Catalog# GFP-1020, chicken polyclonal	1:1,000
NT	Synthetic peptide (human) Neurotensin (Glu-Leu-Tyr-Glu-Asn-Lys-Pro-Arg-Arg-Pro-Tyr-Ile-Leu) coupled to bovine thyroglobulin with glutaraldehyde	ImmunoStar (Hudson, WI), Catalog# 20072, Rabbit polyclonal	1:1,000
pSTAT3	Synthetic phosphopeptide of sequence ADPGSAAPyLKTKFIC corresponding to the amino acid residues flanking Tyr705 (lowercase y) of mouse STAT3	Cell Signaling (Danvers, MA), Catalog# 9131, Rabbit polyclonal	1:1,000
c-Fos	Synthetic peptide (SGFNADYEASSSRC) corresponding to amino acids 4–17 of human c-Fos	CALBIOCHEM (Gibbstown, NJ), Catalog# PC38, Rabbit polyclonal	1:10,000
FG	4-[(E)-2-(4-carbamimidoylphenyl)ethenyl]-3-hydroxybenzenecarboximidamide (Hydroxystilbamidine)	Chemicon, Catalog# AB153, Rabbit polyclonal	1:1,000
CTb	Cholera toxin subunit B (MIKLKFGVFFTVLLSSAYAHGTPQNITDLCAEYHNTQIHTLNDKIFSYTESLAGKREMAIITFKNGATFQVEVPGSQHIDSQKKAIERMKDTLRIAYLTEAKVEKLCVWNNKTPHAIAAISMAN)	List Biological Laboratories, Catalog# 7032A6, Goat polyclonal	1:2,000
MCH	Asp-Phe-Asp-Met-Leu-Arg-Cys-Met-Leu-Gly-Arg-Val-Tyr-Arg-Pro-Cys-Trp-Gln-Val	Phoenix Pharmaceuticals, Catalog# H-070-47, Rabbit polyclonal	1:10,000
Orexin	19 amino acids peptide mapping within amino acids 30–80 of human orexin	Santa Cruz Biotechnology, Catalog# sc-8070, Goat polyclonal	1:1,000
Nesfatin-1	VPIDVDKTKVHNVEPVESARIEPPDTGLYYDEYLKQVIEVLETDPHFREKLQKADIEEIRSGRLSQELDLVSHKVRTRLDEL	Phoenix Pharmaceuticals, Catalog# H-003-22, Rabbit polyclonal	1:1,000

Table 2

a. Colocalization of LHA MC4R-GFP with NT

NT	GFP	Double-labeled	% Double-labeled/GFP
333.7 ± 15.1	104.3 ± 4.6	77.7 ± 5.9	74.4 ± 4.4

b. Colocalization of LHA MC4R-GFP with pSTAT3

pSTAT3	GFP	Double-labeled	% Double-labeled/GFP
371.3 ± 23.9	103.7 ± 9.3	83.0 ± 12.1	79.3 ± 4.9

Values represent estimates of mean counts of cells ± SEM. **Table 2a**. To enhance labeling of NT in cell bodies, the MC4R-GFP mice (n=3) were treated with colchicine 48 hours prior to perfusion and 30 um 1/5 brain sections were processed for double fluorescent IHC for NT and GFP. **Table 2b**. Overnight fasted MC4R-GFP mice (n=3) were received IP injection of letpin (5mg/Kg) 2 hours prior to perfusion and 30 um 1/5 brain sections were processed for double fluorescent IHC for NT and GFP.

Table 3

Influence of MTII and letpin on c-Fos activation of LHA orexin neruons

Time	Drug	Orexin+ Cells	Double c-Fos/Orexin Cells	% of c-Fos on Orexin
ZT8	Saline	610.7 ± 13.4	100.3 ± 12.3	16.5 ± 2.4
	MTII	630.7 ± 30.7	208.0 ± 5.0	33.2 ± 2.3**
	Leptin	622.7 ± 14.1	189.7 ± 19.7	30.1 ± 2.6*
ZT20	Saline	589.3 ± 52.5	275.7 ± 40.8	46.7 ± 5.7
	MTII	611.3 ± 72.2	333.3 ± 58.2	53.7 ± 3.6
	Leptin	646.3 ± 61.9	355.0 ± 42.2	54.8 ± 2.7

Values represent estimates of mean counts of cells ± SEM. The mice received injection of saline, MTII (3mg/Kg) and letpin (5mg/Kg) at two different time points of ZT6 and ZT18 and perfuse, respectively, were perfused 2 hours latter (ZT8 and ZT20, respectively) with 4% PFA and brains were cut into 5 series of 30 um sections (n=3 per group). Brain sections were then processed for double IHC for c-Fos and orexin by biotin/avidin-HRP technique. The presented cell numbers is from three consecutive sections that mainly expressed by orexin neurons.

* $p<0.05$.

** $p<0.01$ compared to saline-injected group.